



Relating laboratory and geophysical well log petrophysical properties in carbonate reservoirs of Southeast Brazil

Abel Carrasquilla, Christiane de Abreu, Paula Almeida & Fernanda Tavares, UENF, Macaé - RJ, Brasil

Copyright 2017, SBGf - Sociedade Brasileira de Geofísica

This paper was prepared for presentation during the 15th International Congress of the Brazilian Geophysical Society held in Rio de Janeiro, Brazil, 31 July to 3 August, 2017.

Contents of this paper were reviewed by the Technical Committee of the 15th International Congress of the Brazilian Geophysical Society and do not necessarily represent any position of the SBGf, its officers or members. Electronic reproduction or storage of any part of this paper for commercial purposes without the written consent of the Brazilian Geophysical Society is prohibited.

Abstract

This petrophysical study characterized a carbonate reservoir located in post salt layer in Campos Basin using geological information, geophysical well logs and laboratory data. Based on density, neutron and sonic logs, different approaches were employed to determine the porosity. In the same way, nuclear magnetic resonance (NMR) log was also utilized to evaluate the porosity and the permeability using different methods. Afterwards, all these parameters were compared between them and with laboratory experimental data. Thus, the results show that to estimate porosity is much more simple than to evaluate permeability, because porosity is well determined with good fit in a multiple linear regression and for permeability a good fit is only achieved with a multiple polynomial regression.

Introduction

This study was performed in a carbonate reservoir of Campos Basin, which is located along the continental shelf of Southeast Brazil (Figure 1). This basin covers an area of approximately 100.000 km², corresponds to the main oil province of Brazil, comprising approximately 80% of the country's oil reserves. It is a typical passive margin basin that started with basaltic extrusion during the Lower Cretaceous above Precambrian crystalline rocks. It evolved tectonically into a rift environment with predominant shallow lacustrine sedimentation, followed by a siliciclastic and evaporitic transitional phase that was linked up to the Southern Atlantic Ocean opening. This tectonic-sedimentary phase persisted until the beginning of middle Cretaceous (Figure 2). An open marine environment developed about 112 million years ago (Early Albian) and still persists today. It started with shallow water carbonate deposition followed by predominantly deep-water siliciclastics. The origin and evolution of this basin are associated with disruption of Gondwana and subsequent opening of the South Atlantic. Hydrocarbon reservoirs occur throughout almost the entire stratigraphic column of this basin, being that the main sequences comprise fractured basalts, coquinas, turbidites, and carbonate rocks. The reservoirs of interest in this work were formed during the Albian, when marine conditions prevailed in giving rise to a carbonate platform of restricted marine basin phase,

yielding the Macaé Group (Figure 3). This group comprises carbonate ramp deposits, containing rocks of various textures such as porous grainstones and packstones, and mudstones of outer platform. The carbonate reservoir addressed in this study has three zones being called, from the youngest to the oldest, as packstone, grainstone and cemented grainstone. The grainstone is considered the reservoir in this oilfield because has the higher values of porosity and permeability (Bruhn et al., 2003).

Among the many physical parameters of an oil and gas reservoir, porosity and permeability are the main factors that determine its storage capacity. However, a very heterogeneous porosity usually occurs within carbonate reservoirs at various scales, from large vugs to small inter-particles, making complex the construction of geological models. These porosity distributions become more intricate even when dissolution and diagenesis processes create secondary porosity. However, high porosity of carbonates allows high capacity hydrocarbon accumulations in these types of reservoirs, which results in high oil production around the world. In that respect, it is thus great interest in studying carbonate reservoirs (Lucia, 2007).

Rock porosity is obtained by direct, as laboratory experiments on core samples, or indirect measurements, as well as logs. Determining porosity through logs is not easy and immediate task, because, usually, a single log is unable to provide a reliable estimate, because they are dependent on various interaction forms between lithology, fluid type, porous geometry and physical properties (Abreu, 2015). Therefore, it is common to use more than one log, for the purpose to reach a better estimation of porosity (Table 1).

In the case of permeability, this parameter is often assessed in the laboratory from reservoir core samples or evaluated from well test data, which are normally only available from a few wells in an oilfield. But, almost all wells are logged and to derive permeability from logs many approaches exist. Thus, NMR log has the ability to estimate formation permeability based on a combination of theoretical and core-based models that suggest that it grows with increasing porosity and pore size. With this log the permeability is calculated from the spectral-porosity measurements using different relationships (Table 2) created from these models (Tavares, 2015).

Method

To develop this work, the initial data set of caliper (CAL), gamma ray (GR), density (RHOB), resistivity (Rt), neutron porosity (NPHI) and sonic (Δt) basic logs, along with the NMR log, were plotted and analyzed. Thereafter, different

porosity values were calculated and plotted using the equations shown in the Table 1, as also, compared with porosity experimental data. According to these results, a multiple linear regression, that includes all the porosity approaches mentioned above, was produced to accomplish a better fit with the laboratory data.

For the permeability, the procedure was very similar to the porosity. Foremost of all, different permeability values were computed and plotted using the equations presented in the Table 2, as also, compared with permeability laboratory data. Having in hand such results, a multiple polynomial regression, that includes all the permeability approaches mentioned before, was made to achieve a better adjust to the observational data.

Results

Track 4 of Figure 4 shows the different types of porosity calculated with the equations shown in Table 1, with ϕ_t (black curve), ϕ_{nmr} (red curve) plotted together with the values measured in the laboratory (ϕ_{lab}) at blue points. Visually, it is observed for both ϕ_t and ϕ_{nmr} not fit well ϕ_{lab} , appearing above or below these experimental data. Because of this bad estimate of this parameter, we resolved to execute an assessment that considers various porosity values through a multiple linear regression $\phi_{regression}$. Figure 5 shows between tracks 1 to 4 various methods to estimate porosity (ϕ_{rhob} , ϕ_{nphi} , $\phi_{\Delta t}$ and ϕ_{nmr}), and $\phi_{regression}$ in the track 5, which uses a combination of these four previous porosities as shown in Table 1. It can be clearly seen a better adjustment of ϕ_{lab} values with $\phi_{regression}$.

Regarding permeability, Figure 6 shows in track 5 the permeability k_{lab} measured in laboratory (blue points). At the same time, we observed k_{coates} (black curve), k_{sdr} (green curve) and k_{timur} (red curve), all calculated with the equations of the Table 2. Although k_{sdr} and k_{timur} have a better fit than k_{coates} as shown in tracks 1 to 3 of Figure 7, all are far from a good fit with k_{lab} . Because of that, we tried a regression using these previous estimates as input. By doing this, we found that simple linear regression does not give a good fit (not shown in figure) as to as a multiple polynomial regression $k_{regression}$, which adjusts well k_{lab} as shown in track 4 (Figure 7).

Conclusions

Our study explored a data set of a carbonate reservoir in Campos Basin, using a joint data interpretation of logs, laboratory core rocks and geological information to assess petrophysical parameters, determining thus the reliability in porosity and permeability estimates. Among evaluations of porosity, $\phi_{\Delta t}$ showed the worst of all, as to multiple linear regression $\phi_{regression}$ was better, which combines ϕ_{rhob} , ϕ_{nphi} , $\phi_{\Delta t}$ and ϕ_{nmr} estimates. Moreover, as k_{timur} , k_{coates} and k_{sdr} permeability individual assessments did not show a good fit with k_{lab} , a combination of the three proved to be a good fit in a multiple polynomial regression $k_{regression}$. Therefore, this work has established that the porosity estimation is much simpler than the permeability, because it is determined with good fit in a multiple linear regression and a worthy fit for permeability is

achieved only with a multiple polynomial regression with a second degree. To develop this work, initial data set of basic caliper, gamma ray (GR), bulk density (RHOB), resistivity (RT), neutron porosity (NPHI) and ultrasonic (DT) logs, along with the NMR log were plotted and analyzed. The following were calculated, plotted and compared the values of different porosities calculated on the Table 1 equations and then make a multiple linear regression that includes all the approaches of porosities mentioned above.

Acknowledgments

We thank the Petrobras Carbonate System of Science, Training and Technology (SCTC) by financial resources to develop a research project and by the release the data set. Thanks also to UENF - LENEP for their physical and computational infrastructure.

References

- Abreu, C. 2015. Porosity estimate and classification using geophysical well logs applied to the Albian carbonates of Campos Basin. Master Thesis, UENF, Macae-RJ, 100p. (In Portuguese).
- Alberty, M. 1994. Standard interpretation; part 4-wireline methods, in D. Morton-Thompson and A. M. Woods, Eds., Development Geology Reference Manual: AAPG Methods in Exploration Series 10, p. 180–185.
- Bruhn, C.; Gomes, J.; Lucchese Jr., C. & Johann, P. 2003. Campos Basin: reservoir characterization and management-historical overview and future challenges. Offshore Technology Conference. OTC 15220.
- Coates, G.; Xiao, L. & Prammer, M. G. 1999. NMR logging: principles and applications. Halliburton Energy Services, Gulf Professional Publishing, Houston, 253p.
- Lucia, J. 2007. Carbonate reservoir characterization: an integrated approach. Springer - Verlag Berlin Heidelberg, 343 p.
- Scott, H.; Wraight, P.; Thornton, J.; Olesen, J.; Hertzog, R.; McKeon, D.; DasGupta, T. & Albertin, I. 1994. Response of a multidetector pulsed neutron porosity tool. Transaction of the SPWLA 35th Annual Logging Symposium, Tulsa, Oklahoma, USA, paper J.
- Schlumberger. 1998. Searching for oil and gas in the land of giants. Buenos Aires, 149 p.
- Schlumberger. 2013. Log interpretation charts. Educational Services. USA, 306 p.
- Tavares, F. 2015. Comparative study of the different estimates of permeability from well logs in carbonate reservoirs. Graduate thesis, UENF, Macae-RJ, 98 p. (In Portuguese).
- Timur, A. 1968. An investigation of permeability, porosity, and residual water saturation relationships for sandstone reservoirs. The Log Analyst IX, SPWLA, v.ix, no.4, a.2.
- Wyllie, M.R.J., Gregory, A.R., and Gardner, L.W. 1956. Elastic wave velocities in heterogeneous and porous media. Geophysics 21(1):41-70.

Table 1. Summary of porosity estimates from logs.

Logs	Required data	Formula	Reference
Density	Matrix (ρ_{ma}) and fluid (ρ_{fl}) densities	$\phi_{rhub} = \frac{\rho_b - \rho_{ma}}{\rho_{fl} - \rho_{ma}}$	Schlumberger (2013)
Neutron	Calibration of the tool with known samples	ϕ_{nphi}	Scott et al. (1994)
Sonic	Matrix (Δt_{ma}) and fluid (Δt_{fl}) transit times	$\phi_{\Delta t} = \frac{\Delta t - \Delta t_{ma}}{\Delta t_{fl} - \Delta t_{ma}}$	Wyllie et al. (1956)
Density + Neutron	Matrix and fluid densities for density log and calibration for neutron log	$\phi_t = \sqrt{\frac{\phi_{rhub}^2 + \phi_{nphi}^2}{2}}$	Alberly (1994)
NMR	Hydrogen index using relaxation times T_1 and T_2	ϕ_{nmr}	Coates et al. (1999)
Regression	$\phi_{rhub} + \phi_{nphi} + \phi_{\Delta t} + \phi_{nmr}$	$\phi_{regression} = -0.007 + 0.407\phi_{rhub} + 0.191\phi_{nphi} + 0.051\phi_{\Delta t} + 0.303\phi_{nmr}$	Abreu (2015)

Table 2. Summary of permeability (mD) estimates from logs.

Logs	Required data	Formula	Referência
Rssistivity + porosity logs or NMR	$\phi_t, S_{wirr}, a_1 = 10^4, b_1 = 4.4$ and $c_1 = 2$	$k_{timur} = a_1 \frac{\phi_t^{b_1}}{S_{wirr}^{c_1}}$	Timur (1968)
NMR	ϕ_{nmr} BVM (mobile fluids), BVI (bound fluids), $a_2 = 4, b_2 = 2$ and $6 < c_2 < 15$	$k_{coates} = \left(\frac{\phi_{nmr}}{c_2} \right)^{a_2} \left(\frac{BVM}{BVI} \right)^{b_2}$	Coates et al. (1999)
NMR	$T_{2gm}, a_3 =$ formation-dependent variable, $b_3 = 4$ and $c_3 = 2$	$k_{sdr} = a_3 \phi_{nmr}^{b_3} T_{2gm}^{c_3}$	Schlumberger (2013)
Regression	k_{timur}, k_{coates} and k_{sdr}	$k_{regression} = -0.007 + 1.1235k_{timur} - 0.0007k_{timur}^2 + 0.7497K_{coates} + 0.0003K_{coates}^2 - 0.1689K_{sdr} + 18.6700K_{sdr}^2$	Tavares (2015)

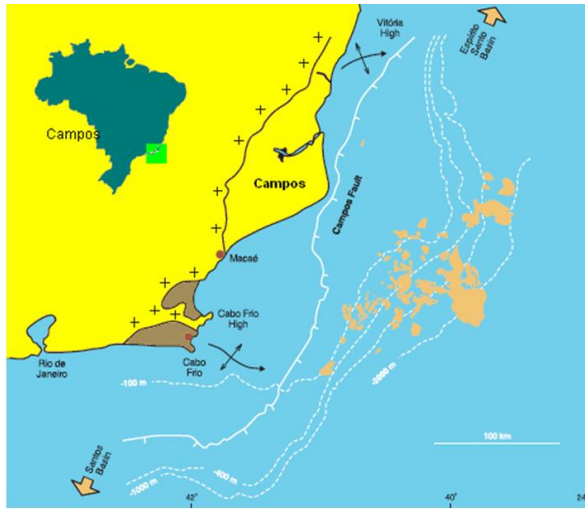


Figure 1. Campos Basin in Southeast Brazil (modified from Bruhn et al., 2003).

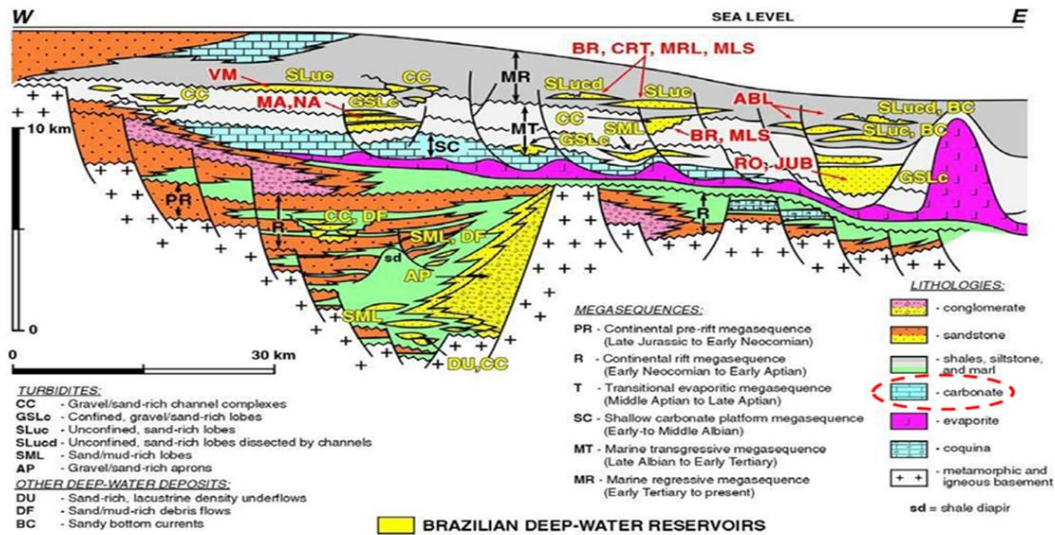


Figure 2. Main reservoirs of Campos Basin. Carbonate reservoirs above salt (evaporites) are the reservoirs studied in this work (modified from Bruhn, 1998).

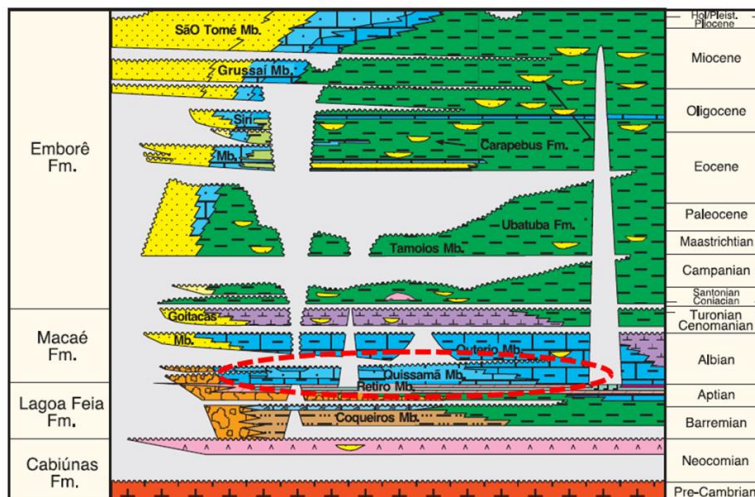


Figure 3. Stratigraphic chart of Campos Basin highlighting Quissamã Formation of Macaé Group (Schlumberger, 1998).

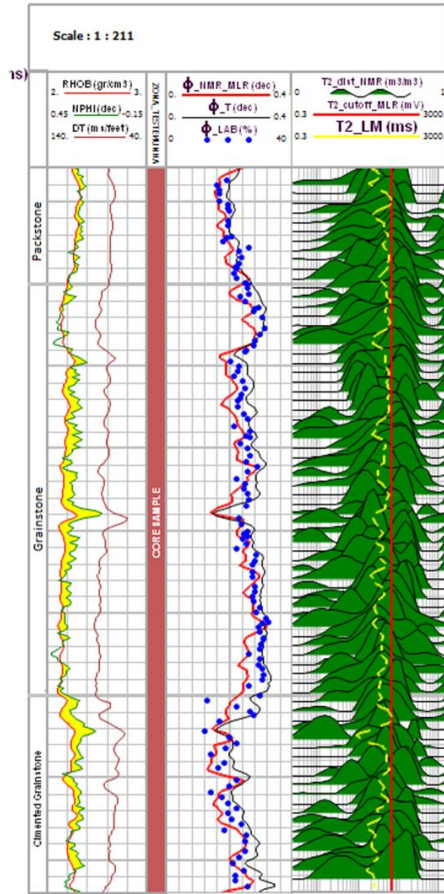


Figure 4. NPHI, RHOB and DT logs, together with porosity estimates and NMR – T_2 distribution, and NMR logs.

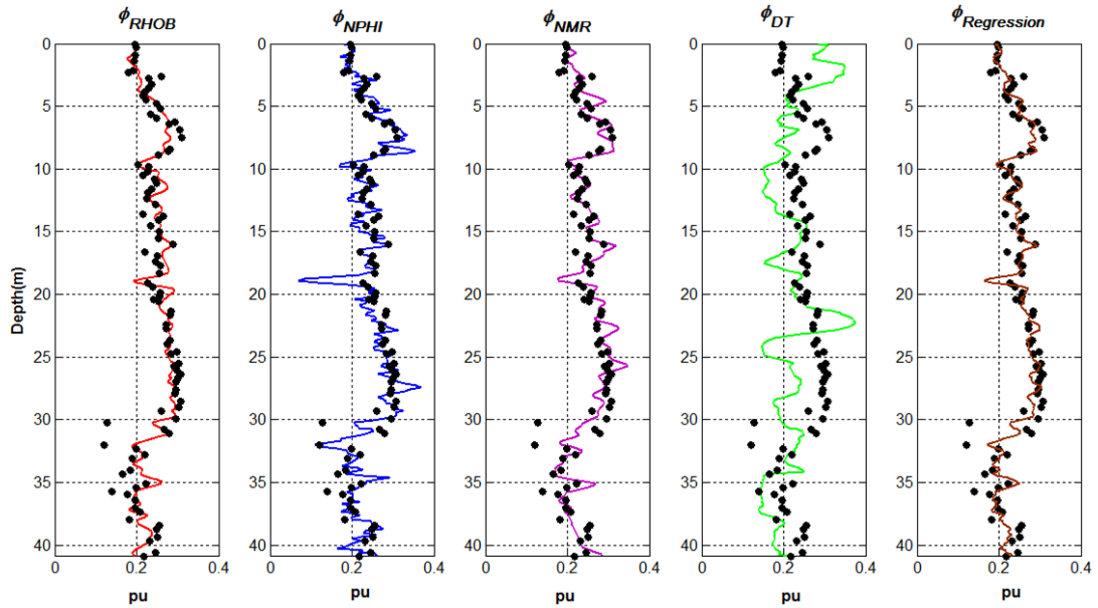


Figure 5. Porosity estimates from RHOB, NPHI, NMR and DT logs.

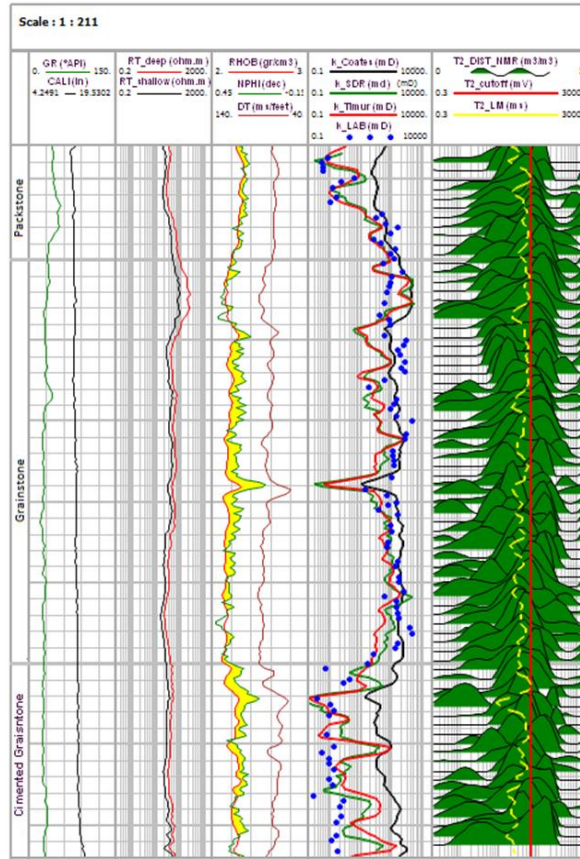


Figure 6. Gamma ray, caliper, resistivity, NPHI, RHOB and DT logs, together with permeability estimates and NMR – T₂ distribution.

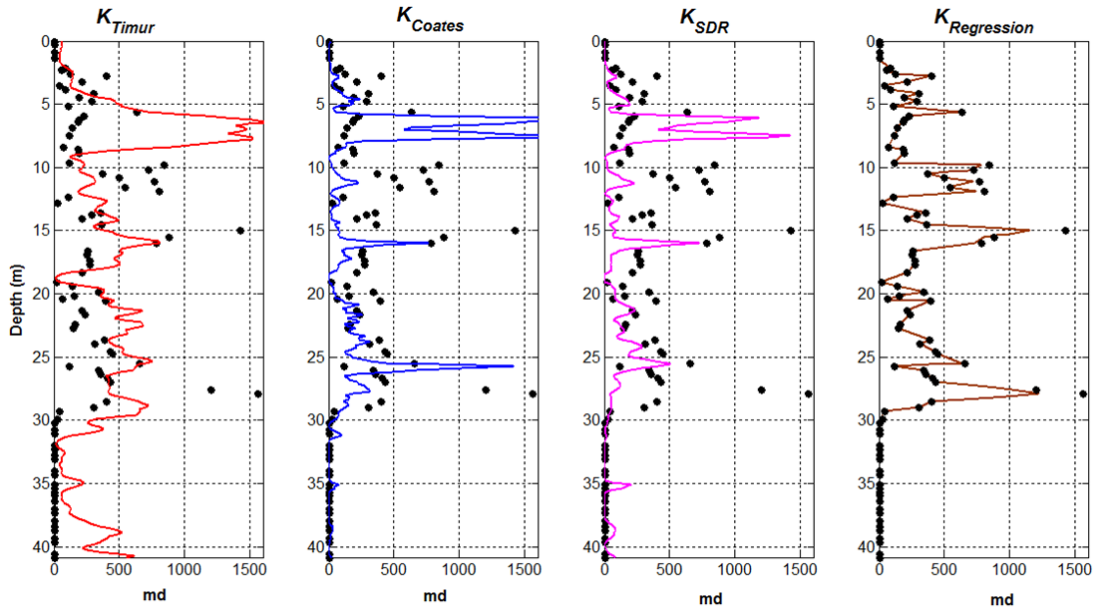


Figure 7. Permeability estimates using Timur, Coates, Schlumberger – Doll Research and Multiple Polynomial Regression approaches.